Journal of the Serbian Chemical Society
JSCS@tmf.bg.ac.rs • www.shd.org.rs/JSCS
*J. Serb. Chem. Soc.* *88* (4) 395–408 (2023)
*JSCS–5634*
*Original scientific paper*
Published 25 March 2023

# Xylose dehydration to furfural using niobium doped *δ*-FeOOH as catalyst

PAULO TADASHI BANNAI CAMPOS[1], MARIANA DE REZENDE BONESIO[1], ANDRÉ LUIZ DIAS LIMA[2], ADILSON CÂNDIDO DA SILVA[2], DAIANA TEIXEIRA MANCINI[1]* and TEODORICO CASTRO RAMALHO[1]**

[1]*Department of Chemistry, Federal University of Lavras 37200-900, Lavras – MG, Brazil and* [2]*Department of Chemistry, Federal University of Ouro Preto, 35400-000, Ouro Preto – MG, Brazil*

(Received 16 March, revised 22 November, accepted 9 December 2022)

*Abstract*: The effect of modification of *δ*-FeOOH with niobium, applied to dehydration reaction of xylose, was evaluated by experimental and theoretical methods. The experimental data confirmed, namely the characteristic peaks in the X-ray diffractometer analysis, that the materials were obtained. Inductively coupled plasma mass spectrometry analysis defined the percentage of Nb as 0 for pure *δ*-FeOOH and 9.5 wt. % (*δ*-FeOOH/Nb) for doped. In relation to obtaining furfural, the doped material presents a conversion improvement of 290 % when compared to pure catalyst. Theoretical calculations were useful in understanding the preferential route of the mechanisms proposed by the obtained potential energy values. To understand the preferred routes, the most favorable position of xylose in relation to *δ*-FeOOH was initially calculated. From this, the conditions favoring furfural formation were calculated based on the routes of the proposed mechanisms and the energy values indicated that the furfural formation is more likely to happen on the doped material.

*Keywords*: feroxyhyte; xylose; furfural; niobium.

## INTRODUCTION

The fossil raw materials dependency can be problematic in the long term, because of scarcity perspective.[1] In this context, the study of renewable raw materials may solve the scarcity issues, also decreases the environmental impacts as the emission of greenhouse gases and the contamination of effluents.[2,3]

Herewith, the vegetable residues generated from agriculture are considered as a renewable material; however, they are used as energy source, through combustion. Nowadays, new forms to increase the added values of these products are being studied using lignin, pentoses and hexoses in the material.[4,5] For example,

* Corresponding authors. E-mail: (*)daianateixeira60@yahoo.com.br; (**)teo@ufla.br
https://doi.org/10.2298/JSC220316085B

furfural is produced from pentoses processing, to be more specific, from xylose. This compound owns numerous applications, as a fungicide, an extracting agent of aromatic compounds for lubricating oils and as diesel.[6] Besides that, furfural would be the basis to produce important compounds as furfuryl alcohol, furan, furoic acid, levulinic acid and tetrahydrofuran.[7]

Currently, homogeneous catalysts are mostly used for the furfural production since these materials own corrosive and dangerous characteristics that damage the production reactors. Associate with this, there is a difficulty of reuse and need for extra steps to catalyst separation, making the process more expensive.[8,9]

Herewith, the study and research of heterogeneous catalysts to the reaction are encouraged. The iron oxides and oxyhydroxides are of great interest since they have natural abundance, chemical stability, corrosion resistance, own attractive physicochemical properties, are easy to obtain and low cost.[10]

Among the iron oxides and oxyhydroxides, feroxyhyte ($\delta$-FeOOH) stands out due to important catalyst characteristics as: ease of obtaining, high surface area, large amount of hydroxyl groups on its surface, and bifunctional catalytic activity. In fact, the superficial groups Fe–OH and its conjugated base Fe–O– act as Brønsted acid and base, respectively,[11] however, the $\delta$-FeOOH has low acid character. Thus, the catalyst modification with other metals may be an alternative to improve these properties.

The modifications of ferric catalyst with niobium are substantially present in the literature, evidencing the modification effectiveness and thus, the study of $\delta$-FeOOH modified with Nb becomes relevant.[12–14] The catalyst modification may increase the catalytic efficiency and material stability. Understanding behavior of these materials as a catalyst is crucial to keep the reaction yield to desirable levels.

The purpose of this work was to evaluate pure and Nb modified $\delta$-FeOOH, as a catalyst, applied to xylose dehydration reaction to furfural employing theoretical and experimental methods.

## EXPERIMENTAL

General procedure for synthesis of pure and doped material. $\delta$-FeOOH nanoparticles were obtained according to the modified procedure described in the literature.[15,16] The method consists mainly of precipitation of an alcoholic solution of $Fe^{2+}$ with NaOH followed by an oxidation with $H_2O_2$, leading directly to the product. The sample was set as Nb 0 wt. %. The Nb doped $\delta$-FeOOH nanoparticles were similarly obtained, however an alcoholic solution of $NbCl_5$ was added before the precipitation step with NaOH, so the final material would have 10 % in Nb mass. The sample was set as Nb 10 wt. %.

The present iron and niobium in the material were determined by the inductively coupled plasma mass spectrometry technique (ICP-MS) monitoring the $^{57}Fe$ and $^{93}Nb$ isotopes. An ELAN DRC II (Perkin Elmer Life and Analytical Sciences, USA) equipment was used. The spectrometry was conducted using platinum sampled and Skimmer cones, both from Perkin Elmer, and argon 99.999 % (White Martins, São Paulo, Brazil). The surface areas were deter-

mined by Brunauer, Emmett and Taller (BET) technique by $N_2$ adsorption/desorption procedure of 22 points in a gas sorption analyzer AUTOSORB Quantachrome. Crystalline phases were got using a X-ray diffractometer (XRD), Rigaku Geigerflex model, equipped with a graphite diffracted bean monochromator. Silicon was used as external standard; the scan was made in the interval 10–80° ($2\theta$) with CuKα |radiation ($\alpha$ = 0.154056 nm).

The xylose dehydration reaction to furfural was investigated using a stainless-steel tubular reactor of 15 mL keeping the temperature controlled at 140 °C in a glycerol bath thermostat (Marconi model MA159/30Glic). 10 mg of catalyst and 10 mL of xylose 20 g $L^{-1}$ solution were added to the reactor. After the pre-stipulated reaction intervals of 15, 30 and 60 min, the process was immediately interrupted by cooling the reactor in an ice bath. Then, the reaction medium was subjected to centrifugation (FANEM excels II model) by 15 min (250 rpm) and the catalyst was recovered by the supernatant collection.

The quantification of xylose and furfural in the liquid phase, after the reaction was carried out, was performed by HPLC (Agilent, model 1260 infinity II). The chromatography system was equipped with an Aminex HPX-87H column (300×7.8 $mm^2$, Bio-Rad) maintained at 55 °C by an oven with forced air circulation, a refractive index detector for detection of xylose, and an ultraviolet–visible (UV–Vis) detector set at 274 nm for detection of 2-furfuraldehyde. An aqueous sulfuric acid (5 mmol $L^{-1}$) solution was used as the eluent at a constant flow rate of 0.6 mL $min^{-1}$.

The conversion and formation of products from xylose were quantified, using an external calibration curve acquired by the injection of the pure product with known concentrations. Xylose conversion ($X_c$) was calculated as:

$$X_c = 100\frac{\text{Final xylose content, mol}}{\text{Initial xylose content, mol}} \quad (1)$$

In order to better understand the role of δ-FeOOH pure and Nb doped applied to the xylose conversion, a theorical study was made, evaluating the adsorption sites of xylose and the different mechanism reactions.

All calculations are made in Gaussian09 software.[17] The system total energy was calculated using the hybrid method of our own *n*-layered integrated molecular orbital and molecular mechanics (ONIOM).[18,19] The region treated as high level was calculated by the density functional theory (DFT) using 6-31G basis set for carbon, oxygen and hydrogen atoms[20–23] and for iron[24] and niobium atoms,[25] the LanL2DZ basis set was chosen. Generalized gradient approximation Perdew–Burke–Ernzerhof (GGA-PBE)[26] was chosen to describe the exchange and correlation term as a function of spin density. The region treated as low level was calculated by molecular mechanical using universal force field (UFF).

For our calculations, we have used a cluster model based on structure previously built and optimized by Lacerda *et al.*,[27] in which, the Nb 0 wt. % was done as described by Drits *et al.*,[28] using DFT under periodic boundary conditions, the functional for the exchange and correlation term was the GGA-PBE,[26] and the projector augmented-wave method, PAW[29], was used with a cutting energy equal to 500 eV. The Nb 10 wt. % structure was made at the same conditions, but due to the similarity in the size of the Fe and Nb atoms, the doping was performed by substitute Fe atoms by Nb atoms of the upper layer of the surface, to produce the material with approximately 10 wt. % (δ-FeOOH/Nb). The substitutions were made in order to leave the dopants equally distributed in surface.

The surface model for both catalysts was generated using a 3×3×2 super cell on the (001) plane, totalizing 288 atoms, in which 72 are iron atoms (6 atoms of Fe were replaced by Nb

atoms in Nb 10 wt. %). The size of surfaces cluster models is sufficient to see the interactions between xylose and $\delta$-FeOOH in QM/MM methods.[30,31]

The xylose has three reaction sites that possibly lead to furfural[32] (marked red in Fig. 1), and, considering these sites, three arbitrary positions for each reaction site were elaborated, totalizing nine different spatial positions. For the input files, VESTA software was used, as it is presented in the Supplementary material to this paper.

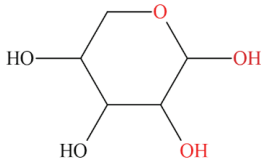


Fig. 1. Xylose reaction sites to furfural.

To evaluate the materials as catalysts, initially we made an adsorption study, combining the different xylose spatial positions and surfaces of Nb 0 and 10 wt. %. For this, the distances between xylose and surfaces ranged from 0.17 to 0.35 nm, with intervals of 0.01 nm, and then we evaluated the most stable combinations of xylose/surfaces. For thermodynamic study the positions and distances, with the minimum energy for each reaction site, were considered.

The xylose dehydration reaction to furfural was thermodynamically studied, optimizing the reaction intermediaries in the presence of Nb 0 and 10 wt. %. The reaction mechanisms used have been proposed in the previous experimental work.[32] The adsorbed/released energy of each step was obtained by applying the equation.

$$\Delta E_{(n)} = (E_{ONIOM/intermediary(n)} - mE_{ONIOM/H_2O}) - E_{ONIOM/xylose} \quad (2)$$

In which $\Delta E_{(n)}$ is the relative energy to the intermediary formation, n is the identification of the associated intermediary, $m$ is the number of free water molecules present in the system, $E_{ONIOM/H_2O}$ is the energy of free water molecule and $E_{ONIOM/xylose}$ is the xylose potential energy on the catalyst.

## RESULTS AND DISCUSSION

ICP–MS technique was used to quantify niobium as the catalyst. Thus, it was determined that the materials Nb 0 and 10 wt. % have 0.00 and 9.50 wt. % of Nb, respectively. On the other hand, the amount of iron present decreased from 63.4 in Nb 0 to 55.1 % in Nb 10 wt. %, respectively. The adsorption $N_2$ isotherms for both catalysts are IV type, showing interparticle mesoporosity. The total pore volume of Nb 0 and 10 wt. % was 0.27 and 0.16 $cm^3\ g^{-1}$, respectively. The estimated specific surface area of Nb 0 and 10 wt. % were 99 and 73 $m^2\ g^{-1}$, respectively, according to the literature (20–300 $m^2\ g^{-1}$).[33]

The X-ray patterns of synthesized compounds are presented in Fig. 2. In both diffractograms feroxyhyte were identified, based on its own characteristics reflection planes, according to the Joint Committee on Powder Diffraction Standards – JCPDS card 13-87. The planes are (100), (101), (102) and (110). In the interval from $2\theta$ 25 to 35°, some shoulders can be observed, and they are assigned to ultrafine iron oxides present in all $\delta$-FeOOH phases.[34] The amorphous contribution rises the Nb incorporation to the material, as seen on Nb 10 wt. % diffractogram.

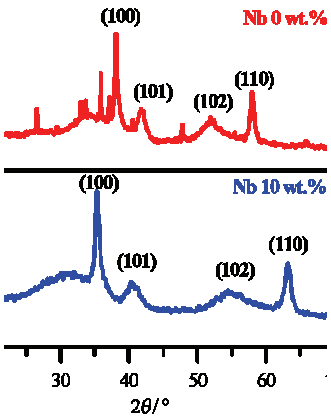


Fig. 2. XRD diffratograms for Nb 0 and 10 wt. %.

To the reflection plane (001), the ratio of relative area from amorphous/ /reflection contribution of δ-FeOOH was estimated at 0.93 and 1.81 for Nb 0 and 10 wt. %, respectively. This fact suggests that the increase from amorphous contribution might be related to a small amount of $Nb^{5+}$ oxyhydroxides formed during the synthesis (JCPDS No 31-928). Both catalysts had particles formed in size 15 nm.

The pure and Nb doped feroxyhyte performances as catalysts were evaluated using the xylose dehydration reaction to furfural as most likely reaction. After one hour of reaction conversion results were obtained as presented in Fig. 3. For Nb 0 wt. % catalyst the conversion rate was about 2.0 %, while for Nb 10 wt. % the conversion was about 7.8 %. Although the conversion rates were relatively low, the catalyst Nb modification presents a conversion improvement of 290 % when compared to pure catalyst. Niobium and its oxides possess Brønsted and Lewis acidity so their higher acidity, when compared to iron oxides, favor heterogeneous catalytic reactions.[13] However, for a superior investigation of the studied material as a catalyst to this reaction, a theoretical approach may contribute to its comprehension.

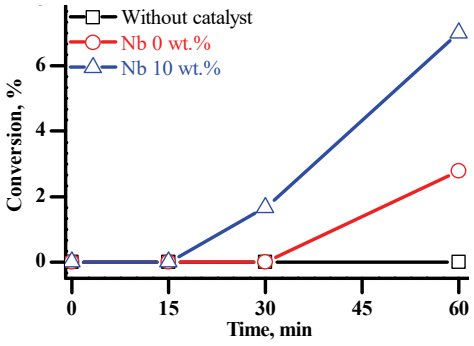


Fig. 3. Xylose conversion kinetic at 140 °C using water as solvent.

In order to understand the reaction mechanism, the ONIOM approach (DFT/UFF) was chosen. With this is possible to see the local structure and better evaluate the regions of interest at low computational demand. Similar structures have shown satisfactory results with this approach.[12,35]

Regarding the computational analysis, Nb 0 and 10 wt. % models were built for a more detailed investigation of xylose dehydration reaction to furfural. To inquire $\delta$-FeOOH catalytic properties the plane (001) was chosen, Fig. 4, corresponding to the one of the most stable catalyst geometry, according to Lacerda.[27]

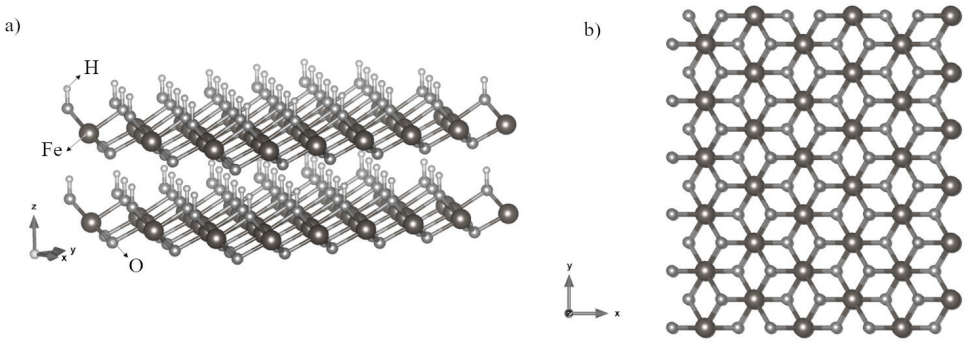


Fig. 4. Nb 0 wt. % system model. The Fe, O and H atoms are pointed out.

The Nb isomorphic substitution in feroxyhyte crystal is due to the similarity in the size of the Fe and Nb atoms. Furthermore, Silva *et al.*,[36] evidenced that the presence of Nb stabilizes the iron oxides structure. There is also the remote possibility of niobium oxide formation on the catalyst surface,[14] but for computational studies only the atoms substitution was considered in super cell building, as shown in Fig. 5.

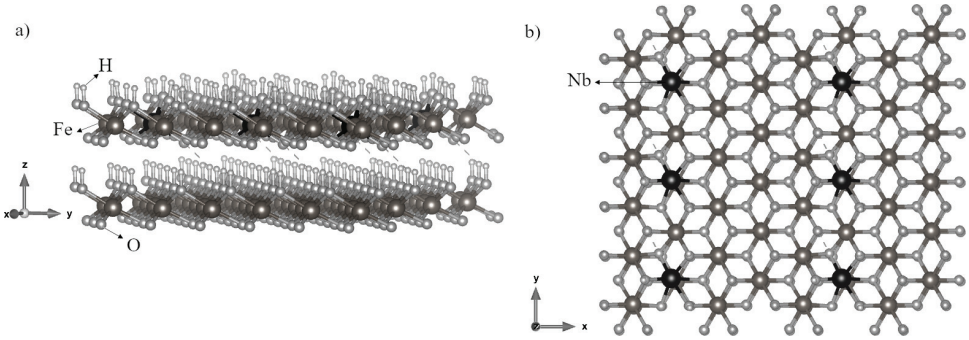


Fig. 5. Nb 10 wt. % system model. The Fe, Nb, O and H atoms are pointed out and Nb atoms are marked black.

The first step to a better understanding dehydration reaction is to know how the catalyst surface interacts with xylose by adsorption tests. Xylose has 3 pos-

sible reaction sites that lead to furfural conversion, Fig. 6, each site leads to a different route reaction, namely routes 1, 2 and 3.

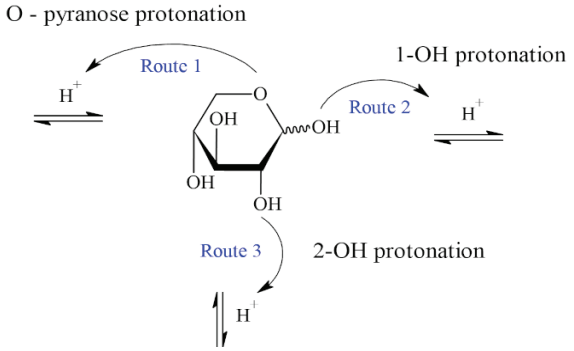


Fig. 6. Possible xylose reaction sites for dehydration reaction to furfural.

Three arbitrary positions for each reaction site were elaborated for adsorption tests (as seen in supplementary material), namely position I, II or III for routes 1, 2 or 3. Combining the possibilities, in total there are 9 different systems for each catalyst.

Fig. 7 shows the best positions and distances chosen after the study of different spatial positions and distances between the catalyst and the sugar. For a superior presentation of the results, potential energy values for distances less than 0.25 nm were omitted, once they were too high. Comparing the results among pure and doped catalyst the resemblance on preference of xylose above feroxyhyte is remarkable. Besides that, the distances are the same or minimally distinct. Fig. 8 shows the most stable positions of xylose on the catalyst for routes 1; 2 and 3, respectively. Table I summarizes all these results.

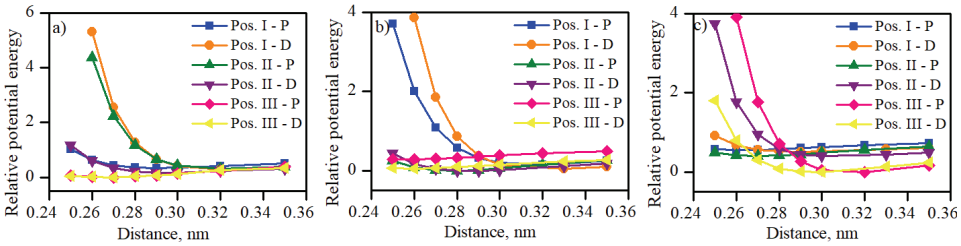


Fig. 7. Calculated potential energy curve for xylose adsorption favoring route: a) 1, b) 2 and c) 3 at different positions. P and D refer to Nb 0 and 10 wt. %, respectively.

The three mechanisms for xylose dehydration to furfural, supported by experimental evidence,[32] are proposed as an acyclic mechanism by the ring opening and two cyclic mechanisms. The difference between them is in the oxygen atom that will be protonated: the ring oxygen (*O*-pyranose), the hydroxyl oxygen in

position 1 (1-OH) or the hydroxyl oxygen in position 2 (2-OH) respectively to the routes 1, 2 and 3, Fig. 8.

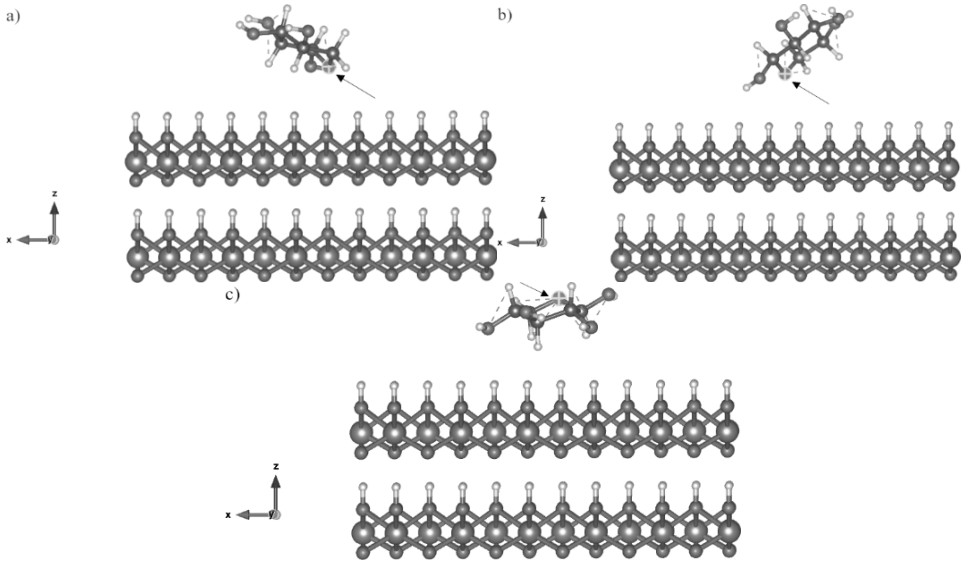


Fig. 8. a), b) and c) refer to routes 1, 2 and 3, respectively. The pointed atom refers to the oxygen belonging to the ring.

TABLE I. Summary of selected positions and distances

| Parameter | Route 1 | | Route 2 | | Route 3 | |
|---|---|---|---|---|---|---|
| | Nb content, wt. % | | | | | |
| | 0 | 10 | 0 | 10 | 0 | 10 |
| Position | III | III | II | II | III | III |
| Distance, nm | 0.27 | 0.27 | 0.28 | 0.28 | 0.32 | 0.30 |

Route 1, Fig. 9a, would occur with the xylose carbonic chain opening resulting in the intermediates reaction formation.

The process finishes with furfural production and three water molecules loss. Routes 2 and 3, Fig. 9b and c, respectively, would occur without breaking of the xylose carbonic chain. The reaction would happen upon three water molecules loss until the furfural formation.[37]

To thermodynamic analysis, reactants, reaction intermediaries and products from xylose dehydration to furfural were optimized, respecting the preferred positions previously determined, for the respective reaction routes described. Fig. 10a shows the relative results of the reaction mechanism thermodynamic analysis in the presence of Nb 0 wt. % catalyst.

The theoretical results do not show the favoring of furfural formation using the pure catalyst, agreeing with experimental results. To xylose protonation in all

routes, an average energy about 77.82 kJ/mol is necessary. By the reaction mechanism to the three routes, is possible to observe that only in the 2C intermediary formation an expressive decrease on the system energy occurs, equivalent to $\Delta E$ = –355.14 kJ/mol, but shortly thereafter there is the energy of adsorption in the other reaction steps.

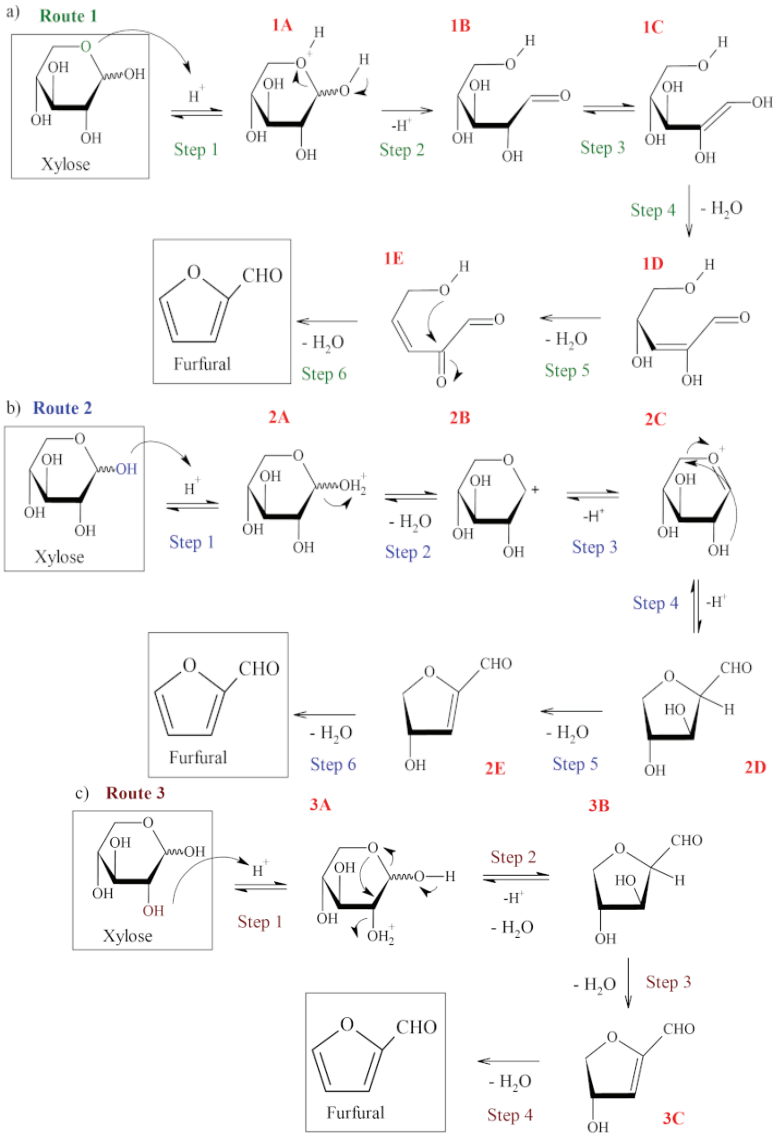


Fig. 9. a) Acyclic reaction mechanism from the *O*-pyranose protonation, route 1; b) cyclic reaction mechanism from the 1-OH protonation, route 2; c) cyclic reaction mechanism from the 2-OH protonation, route 3.

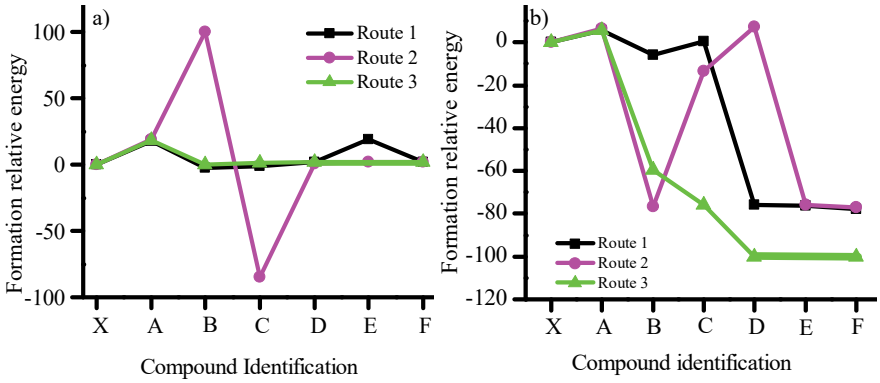


Fig. 10. Relative energy values between reaction steps by: a) Nb 0 and b) 10 wt. % catalyst.

Analyzing the furfural formation in the last step of each route, there is no significant energy difference compared to the other steps, showing that the formation of the product is unlikely. However, the results for Nb 10 wt. % presented in Fig. 10b demonstrate the favoring of furfural production, especially the route 3. For xylose protonation to occur, a 25.10 kJ/mol energy difference is required. Considering B formation, all routes correspond to an exothermic reaction and observing the values to routes 1, 2 and 3 of $\Delta E$ –25.15, –321.46 and –248.32 kJ/mol, respectively, the last two values being high.

Routes 1 and 2 have the furfural production $\Delta E$ of –322.80 kJ/mol, although route 2 is the least likely to happen since between the intermediaries B and D there is a difference of 351.92 kJ/mol. In energetic terms, route 3 is the one thermodynamically favorable, because after xylose protonation the reaction runs an exothermic path until a minimal energetic level through a release of 418.40 kJ/mol.

It is important to keep in mind that iron oxyhydroxides exist in equilibrium with its conjugated basis, but the low acid character of iron compounds limits its use as a catalyst for dehydration reaction:[38]

$$FeOOH_{(s)} + H_2O_{(l)} \leftrightarrows FeOO^-_{(aq)} + H^+_{(aq)} \quad (3)$$

The modification of iron oxides with niobium might rise the catalytic activity and stability as related by Oliveira and collaborators[12] using computational and experimental studies for iron oxide $\alpha$ phase. Studies conducted by Lacerda[27] had shown that the bond distance between hydrogen and oxygen on feroxyhyte surface to pure and doped systems is slightly distinct. In case of pure catalyst the distance is of 0.097 nm, but for the doped is 0.098 nm and this favor the $H^+$ release, implying the Brønsted acidity rise.

According to Pholjaroen,[39] there is evidence that the xylose dehydration reaction to furfural, using a heterogeneous catalyst, may be favored by one active site, especially the cyclic routes. The Lewis acid sites favor the first conversion

step from xylose to xylulose by isomerization, whereas the Brønsted active sites favor the following dehydration steps.[40] Fig. 11 presents a scheme.

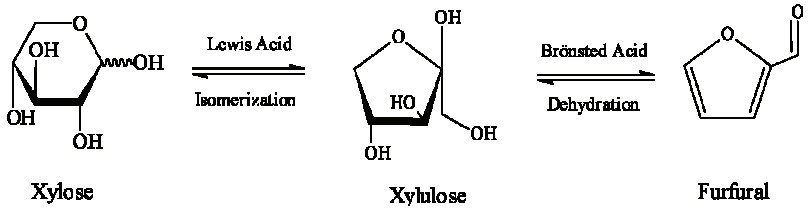


Fig. 11. Xylose Isomerization and dehydratation to furfural.

Niobium and its oxides feature Brønsted and Lewis acidity,[13,14,41] that justifies the superior conversion rate of xylose to furfural for the experimental results and a greater thermodynamic stability presented by the calculations.

## CONCLUSION

Synthesis and characterization of pure δ-FeOOH (Nb 0 wt. %) and doped (Nb 10 wt. %) nanoparticles had proved satisfactory. The doping went close to theoretical value (Nb 9.50 wt. %) and the surface areas are in the literature range.

By conversion rate results, the Nb doped material proved to be more efficient than the pure catalyst, showing a xylose conversion rise of 290 %.

Furthermore, the computational studies indicated that thermodynamic favor use of Nb doped catalyst, related to the pure, when applied to the xylose dehydration reaction to furfural. Hence, route 3 is the most likely reaction route.

The Nb atoms incorporation to δ-FeOOH raises the –OOH groups Brønsted acidity, because it facilitates the $H^+$ release, and the Lewis acid sites formation. Thus, the use of Nb doped materials δ-FeOOH based may be promising in the heterogeneous catalysis field. This paper has supplementary material.

## SUPPLEMENTARY MATERIAL

Additional data and information are available electronically at the pages of journal website: https://www.shd-pub.org.rs/index.php/JSCS/article/view/11693, or from the corresponding author on request.

*Acknowledgements.* The authors would like to thank the Brazilian agencies CNPq (Conselho Nacional de Desenvolvimento Científico e Tecnológico, 409723/2018-5) and FAPEMIG (Fundação de Amparo à Pesquisa do Estado de Minas Gerais, APQ-03226-18), for financial support. Also, this study was financed in part by the Coordenação de Aperfeiçoamento de Pessoal de Nível Superior – Brasil (CAPES) – Finance Code 001, and part of the project involving the Programa de Pós-Graduação da Rede Mineira de Química de Minas Gerais (PPGMQ--MG). This work was supported by University of Hradec Kralove (Faculty of Science, VT2019-2021).

ИЗВОД

## ДОБИЈАЊЕ ФУРФУРАЛА ДЕХИДРАТАЦИЈОМ КСИЛОЗЕ У ПРИСУСТВУ КАТАЛИЗАТОРА *δ*-FeOOH ДОПИРАНОГ НИОБИЈУМОМ

PAULO TADASHI BANNAI CAMPOS[1], MARIANA DE REZENDE BONESIO[1], ANDRÉ LUIZ DIAS LIMA[2], ADILSON CÂNDIDO DA SILVA[2], DAIANA TEIXEIRA MANCINI[1] и TEODORICO CASTRO RAMALHO[1]

[1]*Department of Chemistry, Federal University of Lavras 37200-900, Lavras – MG, Brazil u* [2]*Department of Chemistry, Federal University of Ouro Preto, 35400-000, Ouro Preto – MG, Brazil*

Ефекат модификације *δ*-FeOOH ниобијумом, примењен на реакцију дехидратације ксилозе, испитиван је експерименталним и теоријским методама. Експериментално је потврђено да су материјали добијени на основу карактеристичних рефлексија применом дифракције X-зрачења на праху. Масеном спектрометријом са индуктивно спрегнутом плазмом је одређен садржај Nb и то 0 за чист *δ*-FeOOH и 9,5 мас. % (*δ*-FeOOH/ /Nb) за допиран. Када се прати добијање фурфурала, допирани материјал показује побољшање конверзије од 290 % у поређењу са чистим катализатором. Теоријски прорачуни су омогућили разумевање најповољнијег реакционог пута за механизме предложене на основу вредности потенцијалне енергије. Да би се објаснили најповољнији реакциони путеви, најпре је израчуната најповољнија позиција ксилозе у односу на *δ*-FeOOH. Затим је на основу реакционих путева предложених механизама израчунато када је фаворизовано формирање фурфурала и добијене енергетске вредности указују на то да је већа вероватноћа формирања фурфурала на допираном материјалу.

(Примљено 16. марта, ревидирано 22. новембра, прихваћено 9. децембра 2022)

REFERENCES

1. D. Kumar, B. Singh, J. Korstad, *Renew. Sust. Energ. Rev.* **73** (2017) 654 (https://doi.org/10.1016/j.rser.2017.01.022)
2. G. Toscano, G. Riva, E. Foppa Pedretti, D. Duca, *Biomass Bioenergy* **35** (2011) 3139 (https://doi.org/10.1016/j.biombioe.2011.04.010)
3. L. Kuznetsova, L. Zabodalova, N. Yakovchenko, M. Domoroshchenkova, *Energy Procedia* **95** (2016) 230 (https://doi.org/10.1016/j.egypro.2016.09.057)
4. T. Forster-Carneiro, M. D. Berni, I. L. Dorileo, M. A. Rostagno, *Resour. Conserv. Recycl.* **77** (2013) 78 (https://doi.org/10.1016/j.resconrec.2013.05.007)
5. P. L. de Hoyos-Martínez, X. Erdocia, F. Charrier-El Bouhtoury, R. Prado, J. Labidi, *Waste Manage.* **80** (2018) 40 (https://doi.org/10.1016/j.wasman.2018.08.051)
6. P. Kubelka, F. Munk, *Zeitsch. Tech. Phys.* **12** (1931) 593 (http://www.graphics.cornell.edu/~westin/pubs/kubelka.pdf)
7. G. Machado, S. Leon, F. Santos, R. Lourega, J. Dullius, M. Mollmann, P. Eichler, *Nat. Resour.* **07** (2016) 115 (http://dx.doi.org/10.4236/nr.2016.73012)
8. A. Chatterjee, X. HU, F. L. Y. Lam, *Fuel* **239** (2019) 726 (https://doi.org/10.1016/j.fuel.2018.10.138)
9. C. Garcia-Sancho, I. Agirrezabal-Telleria, M. B. Guemez, P. Maireles-Torres, *Appl. Catal., B* **152** (2014) 1 (https://doi.org/10.1016/j.apcatb.2014.01.013)
10. R. K. Pal, S. Pradhan, L. Narayanan, V. K. Yadavalli, *Sensors Actuators, B* **259** (2018) 498 (http://dx.doi.org/10.1016/j.snb.2017.12.082)
11. P. Chen, K. Xu, X. Li, Y. Guo, D. Zhou, J. Zhao, X. Wu, C. Wu, Y. Xie, *Chem. Sci.* **5** (2014) 2251 (https://doi.org/10.1039/C3SC53303D)
12. L. C. A. Oliveira, F. Zaera, I. Lee, D. Q. Lima, T. C. Ramalho, A. C. Silva, E. M. B. Fonseca, *Appl. Catal., A* **368** (2009) 17 (https://doi.org/10.1016/j.apcata.2009.08.001)

13. H. S. Oliveira, L. D. Almeida, V. A. A. De Freitas, F. C. C. Moura, P. P. Souza, L. C. A. Oliveira, *Catal. Today* **240** (2015) 176 (http://dx.doi.org/10.1016/j.cattod.2014.07.016)
14. A. L. D. Lima, D. C. Batalha, H. V. Fajardo, J. L. Rodrigues, M. C. Pereira, A. C. Silva, *Catal. Today* **344** (2020) 118 (https://doi.org/10.1016/j.cattod.2018.10.035)
15. L. V. C. Lima, M. Rodriguez, V. A. A. Freitas, T. E. Souza, A. E. H. Machado, A. O. T. Patrocínio, J. D. Fabris, L. C. A. Oliveira, M. C. Pereira, *Appl. Catal., B* **165** (2015) 579 (http://dx.doi.org/10.1016/j.apcatb.2014.10.066)
16. M. C. Pereira, E. M. Garcia, A. Cândido da Silva, E. Lorençon, J. D. Ardisson, E. Murad, J. D. Fabris, T. Matencio, T. de Castro Ramalho, M. V. J. Rocha, *J. Mater. Chem.* **21** (2011) 10280 (https://doi.org/10.1039/C1JM11736J)
17. *Gaussian 16, revision C.01*, Gaussian, Inc., Wallingford, CT, 2016 (https://gaussian.com/gaussian16/)
18. L. W. Chung, W. M. C. Sameera, R. Ramozzi, A. J. Page, M. Hatanaka, G. P. Petrova, T. V. Harris, X. Li, Z. Ke, F. Liu, H. B. Li, L. Ding, K. Morokuma, *Chem. Rev.* **115** (2015) 5678 (https://doi.org/10.1021/cr5004419)
19. E. F. F. da Cunha, W. Sippl, T. de Castro Ramalho, O. A. Ceva Antunes, R. B. de Alencastro, M. G. Albuquerque, *Eur. J. Med. Chem.* **44** (2009) 4344 (10.1016/j.ejmech.2009.05.016)
20. T. Costa Martins, T. Ramalho, J. Figueroa-Villar, A. Flores, C. Pereira, *Magn. Reson. Chem.* **41** (2003) 983 (https://doi.org/10.1002/mrc.1299)
21. T. C. Ramalho, M. Bühl, *Magn. Reson. Chem.* **43** (2005) 139 (https://doi.org/10.1002/mrc.1514)
22. A. P. Guimarães, A. A. Oliveira, E. F. F. da Cunha, T. C. Ramalho, T. C. C. França, *J. Biomol. Struct. Dyn.* **28** (2011) 455 (https://doi.org/10.1080/07391102.2011.10508588)
23. T. C. C. França, P. G. Pascutti, T. C. Ramalho, J. D. Figueroa-Villar, *Biophys. Chem.* **115** (2005) 1 (https://doi.org/10.1016/j.bpc.2004.12.002)
24. L. E. Roy, P. J. Hay, R. L. Martin, *J. Chem. Theory Comput.* **4** (2008) 1029 (https://doi.org/10.1021/ct8000409)
25. T. Jian, L. F. Cheung, T.-T. Chen, G. V Lopez, W.-L. Li, L.-S. Wang, *Int. J. Mass Spectrom.* **434** (2018) 7 (https://doi.org/10.1016/j.ijms.2018.08.013)
26. J. P. Perdew, K. Burke, M. Ernzerhof, *Phys. Rev. Lett.* **77** (1996) 3865 (https://doi.org/10.1103/PhysRevLett.77.3865)
27. L. C. T. Lacerda, M. S. Pires, I. S. S. Oliveira, T. C. Telles, A. A. de Castro, S. Corrêa, V. S. Vaiss, T. C. Ramalho, *J. Mol. Model.* **27** (2021) 249 (https://doi.org/10.1007/s00894-021-04864-4)
28. V. A. Drits, B. A. Sakharov, A. Manceau, *Clay Miner.* **28** (1993) 209 (https://doi.org/10.1180/claymin.1993.028.2.03)
29. P. E. Blöchl, *Phys. Rev., B* **50** (1994) 17953 (https://doi.org/10.1103/PhysRevB.50.17953)
30. I. Kumari, N. Kaur, S. Gupta, N. Goel, *J. Mol. Model.* **25** (2019) (10.1007/s00894-018-3899-x)
31. M. Casarin, D. Falcomer, A. Glisenti, M. M. Natile, F. Poli, A. Vittadini, *Chem. Phys. Lett.* **405** (2005) 459 (https://doi.org/10.1016/j.cplett.2005.02.076)
32. H. Rasmussen, H. Sørensen, A. Meyer, *Carbohydr. Res., C* **385** (2013) 45 (https://doi.org/10.1016/j.carres.2013.08.029)
33. R. M. Cornell, U. Schwertmann, *The Iron Oxides: Structure, Properties, Reactions, Occurrences and Uses*, 2nd ed., Wiley-VCH, Weinheim, 2003 (https://doi.org/10.1002/3527602097)

34. C. B. Koch, C. A. Oxborrow, S. Mørup, M. B. Madsen, A. J. Quinn, J. M. D. Coey, *Phys. Chem. Miner.* **22** (1995) 333 (https://doi.org/10.1007/BF00202774)
35. J. B. Lopes Martins, E. Longo, O. D. Rodríguez Salmon, V. A. A. Espinoza, C. A. Taft, *Chem. Phys. Lett.* **400** (2004) 481 (https://doi.org/10.1016/j.cplett.2004.10.150)
36. A. C. Silva, R. M. Cepera, M. C. Pereira, D. Q. Lima, J. D. Fabris, L. C. A. Oliveira, *Appl. Catal., B* **107** (2011) 237 (http://dx.doi.org/10.1016/j.apcatb.2011.07.017)
37. M. J. Antal, T. Leesomboon, W. S. Mok, G. N. Richards, *Carbohydr. Res.* **217** (1991) 71 (https://doi.org/10.1016/0008-6215(91)84118-X)
38. M. Pires, L. Lacerda, S. Corrêa, T. Silva, A. Castro, T. Ramalho, in *Recent Advances in Complex Functional Materials*, Springer, Berlin, 2017, pp. 409–425 (https://doi.org/10.1007/978-3-319-53898-3_16)
39. B. Pholjaroen, N. Li, Z. Wang, A. Wang, T. Zhang, *J. Energy Chem.* **22** (2013) 826 (https://doi.org/10.1016/S2095-4956(14)60260-6)
40. I. Agirrezabal-Telleria, C. García Sancho, P. Maireles-Torres, P. L. Arias, *Chinese J. Catal.* **34** (2013) 1402 (https://doi.org/10.1016/S1872-2067(12)60599-3)
41. J. B. Gabriel, V. Oliveira, T. E. De Souza, I. Padula, L. C. A. Oliveira, L. V. A. Gurgel, B. E. L. Baêta, A. C. Silva, *ACS Omega* **5** (2020) 21392 (https://doi.org/10.1021/acsomega.0c01547).